



ELSEVIER

Contents lists available at ScienceDirect

Continental Shelf Research

journal homepage: www.elsevier.com/locate/csr

Research papers

Recent organic carbon accumulation (~ 100 years) along the Cabo Frio, Brazil upwelling region

Christian J. Sanders^{a,*}, Pedro P. Caldeira^b, Joseph M. Smoak^c, Michael E. Ketterer^{d,2},
 Andre Belem^a, Ursula M.N. Mendoza^a, Livia G.M.S. Cordeiro^a, Emmanoel V. Silva-Filho^a,
 Sambasiva R. Patchineelam^a, Ana Luiza S. Albuquerque^a

^a Universidade Federal Fluminense, Departamento de Geoquímica, Rua Outeiro São João Baptista S/N, Morro do Valonginho, Niterói-RJ 24020-141, Brazil

^b Departamento de Biofísica, Universidade Federal do Rio de Janeiro, Instituto de Biofísica Carlos Chagas Filho, Avenida Carlos Chagas Filho, Rio de Janeiro – RJ 21941-902, Brazil

^c Department of Environmental Science, Policy and Geography, University of South Florida, St. Petersburg, FL 33701, USA

^d Department of Chemistry and Biochemistry, Northern Arizona University, Box 5698, Flagstaff, AZ 86011-5698, USA

ARTICLE INFO

Article history:

Received 4 April 2013

Received in revised form

7 September 2013

Accepted 15 October 2013

Available online 30 October 2013

Keywords:

Sedimentation

Organic sediments

 ^{210}Pb and $^{239+240}\text{Pu}$ geochronology $\delta^{13}\text{C}$

TOC/TN molar ratio

Lateral transport

ABSTRACT

Six sediment cores were obtained from the Cabo Frio shelf region of coastal Brazil to quantify the accumulation of organic carbon in a highly productive upwelling region. The sampled locations, 10–60 km offshore at ~ 100 m water depth, were investigated for excess ^{210}Pb ($^{210}\text{Pb}_{\text{ex}}$) as well as $^{239+240}\text{Pu}$ fallout activities to determine sedimentary dynamics. The $^{210}\text{Pb}_{\text{ex}}$ and $^{239+240}\text{Pu}$ dating models show that the sediment accumulation rates varied substantially throughout this complex hydrodynamic system ($0.8\text{--}5.5\text{ mm yr}^{-1}$). Excess ^{210}Pb and $^{239+240}\text{Pu}$ fluxes indicate lateral transport, with varying intensity along the continental shelf. The stations with the greatest $^{210}\text{Pb}_{\text{ex}}$ and $^{239+240}\text{Pu}$ sediment inventories are also the sites with the highest carbon accumulation rates (CAR). The total organic carbon (TOC) and total nitrogen (TN) contents, along with the $\delta^{13}\text{C}$ results, indicate that the organic matter deposited in this region is mainly of marine origin. The results of this work suggest that lateral transport, with varying intensity along the shelf, contribute to the large quantities of marine plankton buried at specific depositional settings in the Cabo Frio upwelling region ($\sim 1\text{--}8\text{ mol of OC cm}^{-2}\text{ yr}^{-1}$).

© 2013 Elsevier Ltd. All rights reserved.

1. Introduction

The ocean accounts for almost half of the world's net annual photosynthesis, much of which is produced on or near continental shelves (Burone et al., 2011; Muller-Karger et al., 2005; Thunell et al., 2007). Upwelling areas near the continental shelf are known for particularly high primary production rates, as these areas are fueled by the advection of nutrient-rich waters (Blanco et al., 2001; Muller-Karger et al., 2005; Niggemann et al., 2007; Thunell et al., 2007). The upwelled nutrient-rich water either moves across the shelf through lateral circulating processes or is retained shoreward of the shelf break (Jahnke et al., 1990).

Oceanic inputs through wind-driven processes such as eddies associated with boundary currents are typical in coastal upwelling systems (Jahnke et al., 1990; Thunell et al., 2007). These systems are influenced by western boundary currents such as the Brazil Current (BC) along with eddy interactions (Belem et al., 2013). Because the biological productivity and associated high particle fluxes are mostly shoreward of the shelf break, sinking particles tend to accumulate more efficiently in shelf sediments. The burial efficiency of organic carbon (OC) is enhanced by the shallow water column and rapid rate of sediment accumulation (Smoak et al., 1999). The production of OC in these systems is directly influenced by upwelling as the shallow water depths of continental shelves extend to the slope, favoring the production and accumulation of organic-rich sediments (Baumgart et al., 2010; Burone et al., 2011; Niggemann et al., 2007). Many of the physical processes along upwelling regions enhance primary production and facilitate the downward flux of settling particles (Antoine et al., 1996; Fischer et al., 2000). Understanding the processes that control accumulation of OC in sediments from upwelling regions is of significance when characterizing the processes involved in the marine organic carbon cycle (Baumgart et al., 2010; Jahnke et al., 1990).

The objectives of this study are to quantify recent organic carbon accumulation rates through $^{210}\text{Pb}_{\text{ex}}$ and $^{239+240}\text{Pu}$ profiles,

* Corresponding author.

E-mail addresses: christian.sanders@scu.edu.au, zinosanders@yahoo.com (C.J. Sanders).

¹ Current address: Centre for Coastal Biogeochemistry Research, School of Environment, Science and Engineering, Southern Cross University, P.O. Box 157, Lismore, NSW 2480, Australia.

² Current address: Department of Chemistry, Metropolitan State University of Denver, PO Box 173362, Campus Box 52, Denver, CO 80217-3362, USA.

and to indicate the sources of deposited organic matter using total organic carbon measurements (TOC), total nitrogen (TN) and $\delta^{13}\text{C}$. We hypothesize that lateral transport is an important mechanism influencing the organic carbon accumulation rates (CAR) along the Cabo Frio continental shelf. Fluxes and sediment inventories of $^{210}\text{Pb}_{\text{ex}}$ and $^{239+240}\text{Pu}$ are used to examine this hypothesis.

2. Site description

The Cabo Frio upwelling zone is dominated by two principal oceanographic, physiographic and geomorphological systems. One is the Brazil current (BC) which flows along the Brazilian south-eastern coast including an area of active upwelling between Cabo Frio (23°S) and Cabo de Santa Marta (28°S). The other is marked by the upwelling of the South Atlantic Central Water (SACW), both near the coastal zone and over the continental shelf. The continental shelf is characterized by two distinct bathymetric surfaces, one approximately 50 m deep and extending 5 km offshore and a second ranging from 90 and 130 m deep and extending from 5 to 100 km offshore to the shelf break (Campos et al., 2000; Valentin et al., 1987).

The coastal upwelling of the SACW directly influences the maximal primary production near the Cabo Frio shelf break (Burone et al., 2011; Sumida et al., 2005; Yoshinaga et al., 2010), though these events may shift in accordance with climatic factors (Souto et al., 2011) and references therein). The primary productivity in this upwelling zone has been documented to be between 188 and 520 $\text{g m}^{-2} \text{yr}^{-1}$ of organic matter (Burone et al., 2011). This value is in agreement with the primary production values in other upwelling regions of the world (Baumgart et al., 2010; Muller-Karger et al., 2005; Niggemann et al., 2007; Thunell et al., 2007).

3. Materials and methods

3.1. Geophysical survey

The geophysical survey included seismic profiling with an operating frequency of 3.5 kHz using the Geopulse Geoacoustics system. For the echo-character depth calculations, a speed of 1500 m/s

through the sediments was assumed. The high-resolution seismic bathymetric survey covered a total area of 680 km^2 within the framework of SE-NW and NE-SW configurations (Fig. 1). Based on the geophysical survey, six box-cores were collected across the shelf within the 680 km^2 mud bank (Fig. 1), formed by transgressive–regressive events during the Last Glacial Maximum, and favored by the position of the quasi-stationary Cabo Frio eddy. Sediment cores were sub-sampled by using PVC tubes ($\varnothing=10$ cm, 40 cm length). The sediment cores were collected in an attempt to best represent the Cabo Frio upwelling region (~ 100 m depth), where the SACW and BC currents meet (Fig. 1).

3.2. Radionuclide analyses

For $^{210}\text{Pb}_{\text{ex}}$ analyses, sediment cores were sectioned at 1 cm intervals. Sediments from each interval were sealed in 70 mL Petri dishes for at least three weeks to establish secular equilibrium between ^{226}Ra and its daughters ^{214}Pb and ^{214}Bi . Gamma spectrometric measurements were conducted by using a semi-planar intrinsic germanium high purity coaxial detector with 40% efficiency, housed in a lead shield, coupled to a multichannel analyzer. Activities of ^{210}Pb were determined by the direct measurement of 46.5 keV photopeak, while ^{226}Ra activities were obtained by averaging peaks from the daughters ^{214}Pb and ^{214}Bi (295.2 keV, 351.9 keV and 609.3 keV) (Moore, 1984). The excess ^{210}Pb ($^{210}\text{Pb}_{\text{ex}}$) activity was estimated by subtracting the ^{226}Ra from the total ^{210}Pb activity. Samples were counted for at least 86,000 s in identical geometrical cylinders. Self-absorption corrections were calculated following the method of (Cutshall et al., 1983). The sediment accumulation rates (SAR) were obtained through the Constant Initial Concentration (CIC) dating method (Appleby and Oldfield, 1992), as $^{210}\text{Pb}_{\text{ex}}$ was fitted via the least squares procedure and the slope of the log-linear curve was used to calculate the SAR.

For $^{239+240}\text{Pu}$ measurements, the procedures followed were based upon procedures given in (Ketterer et al., 2004) and (Sanders et al., 2010). Dried, pulverized sediment sub-samples of ~ 10 g were dry-ashed overnight at 600 °C for 16 h, and leached in a 40 mL glass vial with 20 mL of 16 M HNO_3 . The leaching was conducted overnight at 80 °C with added ^{242}Pu yield tracer (NIST 4334 g, 44.6 μg). Acid leaching (as opposed to complete

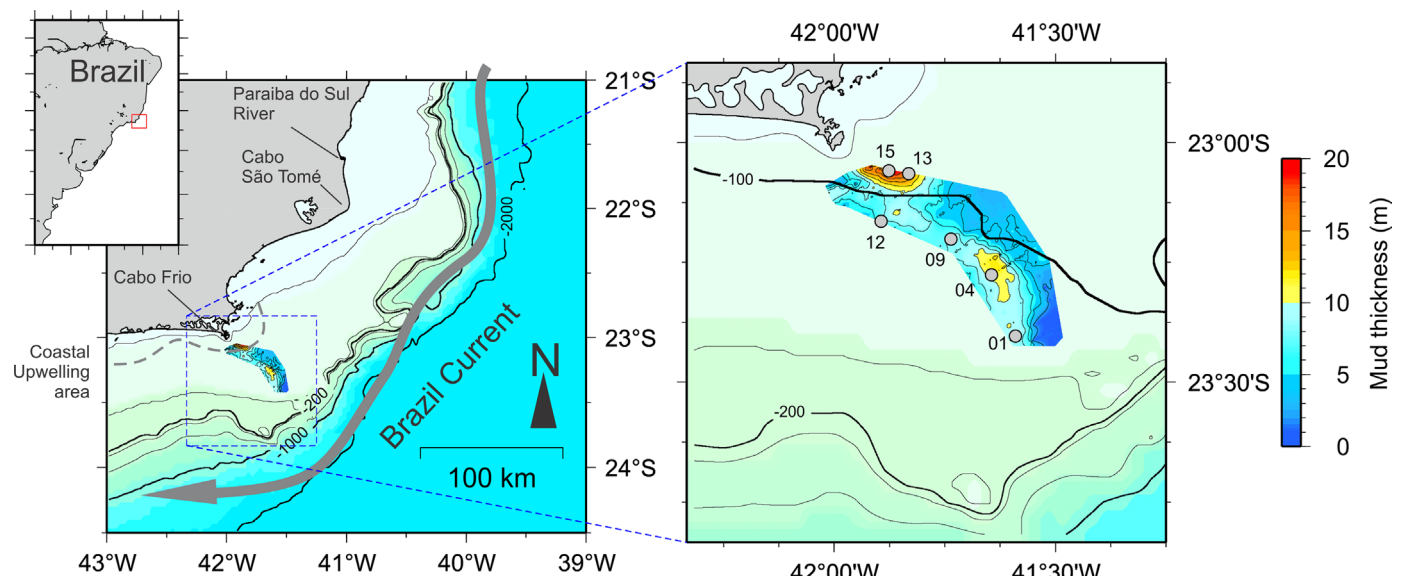


Fig. 1. Study stations along the Cabo Frio continental shelf where the six box-cores were collected.

dissolution with HF) is known to solubilize stratospheric fallout Pu, and there is little possibility that “refractory” HNO₃-insoluble Pu exists in the Brazilian coastal setting. The leachates were diluted to 50 mL, and centrifuged. The supernatant liquid was filtered through a cotton wool plug to remove any remaining particles, and the aqueous solutions were processed with TEVA resin (EI Chrom, Lisle, IL, USA) in order to chemically isolate 1.5 mL Pu fractions in aqueous ammonium oxalate solution (Ketterer et al., 2004; Sanders et al., 2010). The separation procedures eliminate ~99.999% of the U, which can produce ²³⁸U¹H⁺ that interferes with the determination of ²³⁹Pu⁺; a UH⁺ correction factor was measured using a U tuning solution and this factor was used to subtract the small residual contribution from ²³⁸UH⁺ at *m/z* 239. Plutonium determinations were performed using a Thermo X Series II quadrupole ICPMS instrument equipped with an APEX HF desolvating micronebulizer system (ESI Scientific, Omaha, NE, USA). The sample uptake rate was 300 μL min⁻¹. The mass analyzer was operated in a peak-jump mode to monitor ion intensities at ²³⁸U, ²³⁹Pu, ²⁴⁰Pu, and ²⁴²Pu. Detection limits were evaluated through analysis of powdered rock samples (devoid of detectable Pu) as negative controls; a detection limit of 0.02 Bq/kg of ²³⁹⁺²⁴⁰Pu is applicable for samples of nominal 10 g mass. During the course of the study, aliquots of a US Department of Energy control sample (MAPEP 01-S8) were prepared and analyzed. The MAPEP material has an established interlaboratory consensus activity of 78.1 ± 6.3 Bq/kg ²³⁹⁺²⁴⁰Pu; found herein was 79.0 ± 5.7 Bq/kg (average ± standard deviation, *n*=8 independent preparations).

3.3. Sediment profile analyses

A 5-g aliquot from each 1 cm interval was acidified to remove carbonate material, then dried and ground to powder for total organic carbon (TOC), total nitrogen (TN) and δ¹³C analyses using an isotope ratio mass spectrometer (Thermo Finnigan Model Delta Plus XP), following the methods described in (Naidu et al., 2000). From the original wet section, the dry bulk density (DBD) was determined following (Ravichandran et al., 1995). Organic carbon accumulation rates were calculated based on SAR, DBD and TOC contents. The grain-size composition of the fractions with diameters of 0.04–500 μm was analyzed using a 2 g gross weight of sediment and determined with a Cilas[®] 1064 laser analyzer. The samples were analyzed in 0.5 phi intervals.

4. Results

4.1. General sediment characteristics

From the geophysical survey, the sediment layers range from ~1 to ~20 m thick throughout the study area (Fig. 1). There are two isolated deep sediment depositional zones joined along a

100 m isobath. The sediment is the thickest in close proximity to the coast, near Station 15. This area is of lower energy, and a convergence site between the water masses (BC and SACW). The average results for the bulk sediment properties of the six cores in this study are depicted in Table 1. The core profiles may be seen in Supplementary material, Fig. a–f. The outer shelf (Station 1) and inner shelf stations (Stations 13 and 15) show relatively large concentrations of mud at 44.6%, 55.9% and 46.3%, respectively. The Stations towards the center of the shelf (Stations 12, 4 and 09) (Table 1) contain more coarse material with the mass fraction < 63 μm being 24.8%, 26.8% and 32.7%, respectively. The total organic carbon content is approximately 2% along the shelf, being slightly greater towards the center of the transect (Table 1). Carbonate content in the sediment was consistently ca. 20% throughout the study area. The δ¹³C values varied between –21 and –23, being the lowest at Station 9 core. The C/N molar ratio averages varied between 8 and 10. The TN content varied among the different stations (between 0.2% and 0.3%) (Table 1).

4.2. Sediment accumulation

Profiles of the log ²¹⁰Pb_{ex} vs. depth for all six sediment cores are presented in Fig. 2(a–f). The ²¹⁰Pb_{ex} profiles for Stations 1, 4 and 9 suggest that mixing is relatively minor or insignificant at these locations. Physical mixing and/or bioturbation in the superficial layers are evident in the top 3 cm in Stations 13 and 15 (Fig. 2). The ²¹⁰Pb_{ex} profile indicates more intense mixing in Station 12, down to the 7 cm depth (Fig. 2). The ²¹⁰Pb_{ex} data from Station 12, which is on the edge of the large mud depositional area, shows intense physical mixing and/or bioturbation and the lowest sediment accumulation rate of the six cores (Table 2). Excluding Station 12, the sediment accumulation rates were the greatest in the inner shelf (5.5 mm yr⁻¹) and gradually decreased towards the outer shelf (1.1 mm yr⁻¹) (Table 2). From the ²¹⁰Pb dating method employed here (CIC) it is assumed that ²¹⁰Pb_{ex} activity is constant at surface and the sedimentation rate is invariant (Appleby and Oldfield, 1992).

The ²³⁹⁺²⁴⁰Pu activity profiles are presented in Fig. 3. Plutonium is first detected at specific depths in each core and in all cases is continuously present in all overlying intervals. However, there is no consistent activity pattern that resembles the expected atmospheric weapons test deposition history (Ketterer et al., 2004). Therefore, it is not possible to assess a 1963 peak deposition date from these profiles. Nevertheless, material below the first occurrence of ²³⁹⁺²⁴⁰Pu activity represents pre-bomb (that is, prior to 1954 as measurable ²³⁹⁺²⁴⁰Pu activity is anthropogenic and was not introduced into the environment before this date) deposited material. This affixes an upper limit on the sedimentation accumulation rate (SAR) for each core, greater than 3.1 mm yr⁻¹ in the inner shelf to 1.1 mm yr⁻¹ in the outer shelf station (Table 2). The ²³⁹⁺²⁴⁰Pu dates are in agreement with the SAR trends from the ²¹⁰Pb_{ex} geochronologies.

Table 1
Characterization of each core, including core length (cm), water depth (m), δ¹³C (‰), TOC and TN content (mmol g⁻¹), TOC/TN molar ratios, granulometric (mud content, i.e. particles < 63 μm) and dry bulk densities (DBD) (g cm⁻³). Location of each station are as follows: (1) W 41°59'00.00" S 23°40'39.00"; (4) W 42°04'47.00" S 23°28'03.99" (9) W 42°14'01.00" S 23°20'13.99" (12) W 42°29'35.99" S 23°16'40.00" (13) W 42°23'16.99" S.

Station	Length (cm)	Depth (m)	δ ¹³ C	TOC	TN	C:N	DBD	< 63 μm
1	15	142	-21.3 ± 0.4	1.4 ± 0.4	0.2 ± 0.0	8.7 ± 0.5	1.7 ± 0.0	44.6 ± 12.0
4	22	120	-21.2 ± 0.2	2.1 ± 0.2	0.3 ± 0.0	9.3 ± 0.6	1.6 ± 0.1	26.8 ± 8.6
9	19	117	-21.7 ± 0.3	1.9 ± 0.4	0.2 ± 0.0	9.1 ± 0.7	1.6 ± 0.2	32.7 ± 4.5
12	11	87	-21.3 ± 0.2	1.7 ± 0.4	0.2 ± 0.0	8.6 ± 0.9	0.9 ± 0.1	24.8 ± 4.7
13	11	88	-21.3 ± 0.1	1.2 ± 0.2	0.2 ± 0.0	9.2 ± 0.2	1.6 ± 0.0	55.9 ± 6.8
15	15	80	-21.2 ± 0.2	1.7 ± 0.5	0.2 ± 0.1	8.7 ± 0.3	1.0 ± 0.1	46.3 ± 7.8

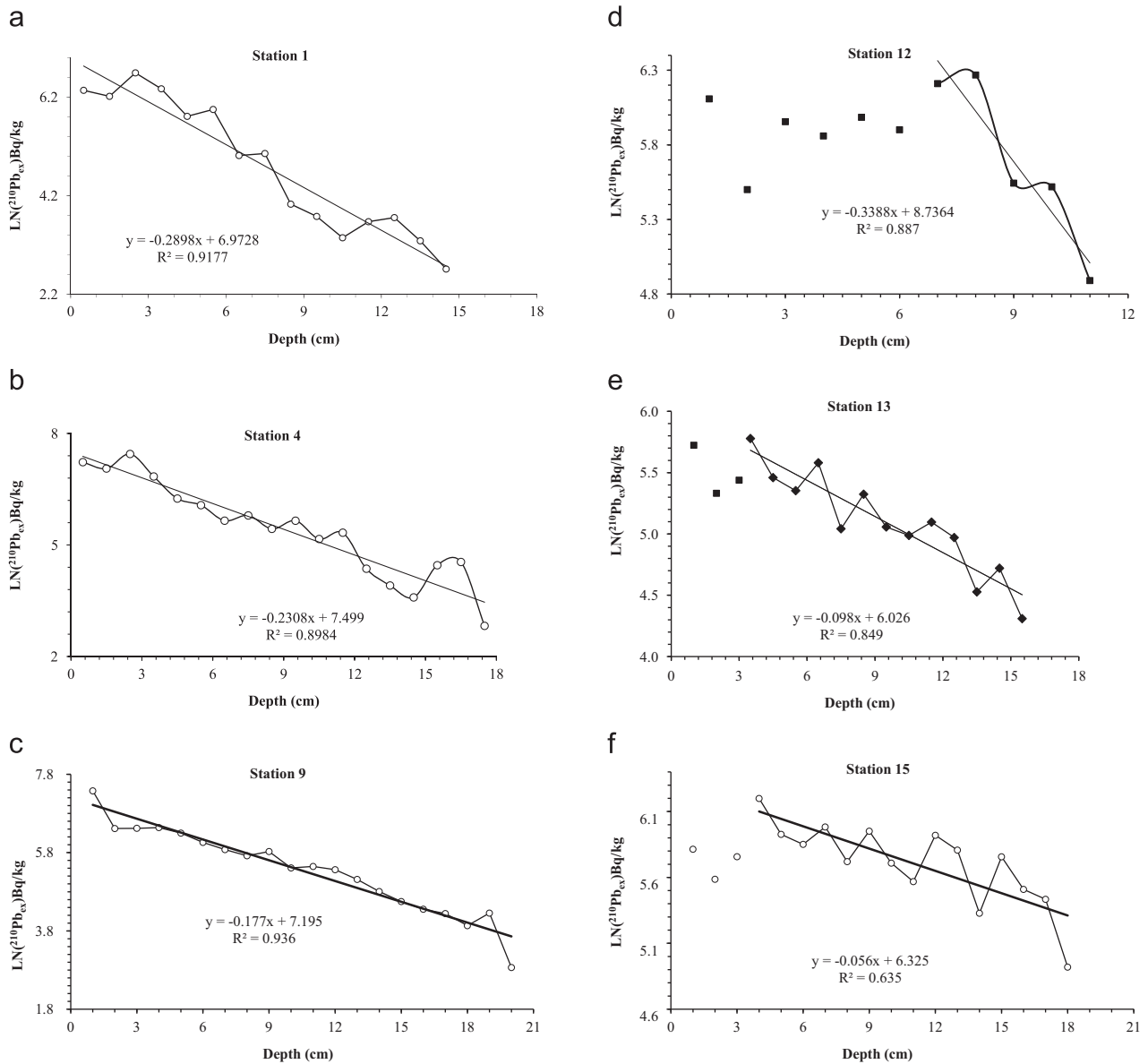


Fig. 2. Log linear profile of $^{210}\text{Pb}_{\text{ex}}$ against depth (the ^{210}Pb and ^{226}Ra counting errors were less than 5%).

Table 2

Radioisotope tracer data; $^{210}\text{Pb}_{\text{ex}}$ inventory (mBq cm^{-2}) affixed to the upper limit 1954; $^{210}\text{Pb}_{\text{ex}}$ flux ($\text{mBq cm}^{-2} \text{yr}^{-1}$) from ~1954; sediment accumulation rates (SAR) (mm yr^{-1}); $^{239+240}\text{Pu}$ flux (mBq cm^{-2}).

Station	$^{210}\text{Pb}_{\text{ex}}$ inventory	$^{210}\text{Pb}_{\text{ex}}$ flux	SAR ^a	$^{239+240}\text{Pu}$ flux	SAR ^b
1	2200	68.3	1.1	0.33	1.1
4	2410	75.0	1.4	0.34	1.9
9	2570	79.8	1.8	0.38	2.5
12	778	24.2	0.9	0.20	0.8 ^d
13	1661	51.5 ^c	3.2	0.31 ^c	> 2.8
15	3829	118.7 ^c	5.5	0.43 ^c	> 3.1

^a $^{210}\text{Pb}_{\text{ex}}$ derived sediment accumulation rates.

^b $^{239+240}\text{Pu}$ derived sediment accumulation rates.

^c Because sediment core depth did not reach 1954, inventories and fluxes are taken from the entire core.

^d Sediment accumulation rate does not consider the apparent large mixed layer.

To investigate the origin of the Pu, and to validate whether or not its source is stratospheric fallout rather than other possible anthropogenic sources (e.g. nuclear power plant accidents), the

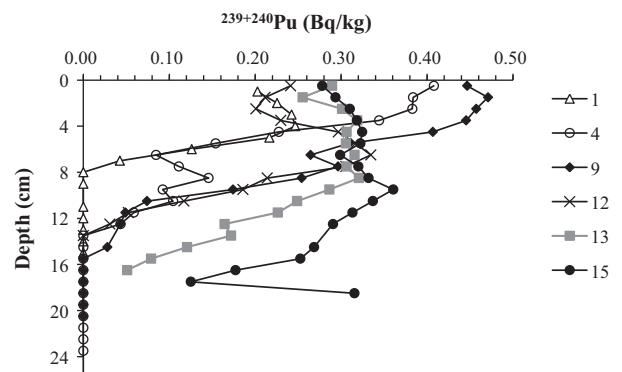


Fig. 3. Activity-depth profiles for $^{239+240}\text{Pu}$.

atom ratio $^{240}\text{Pu}/^{239}\text{Pu}$ was determined along with the $^{239+240}\text{Pu}$ activities. The atom ratios could be determined reliably for most core intervals where the $^{239+240}\text{Pu}$ activity exceeded 0.1 Bq/kg. For the six cores 1, 4, 9, 12, 13, and 15, the $^{240}\text{Pu}/^{239}\text{Pu}$ ratios were 0.190 ± 0.009 ($n=7$), 0.177 ± 0.015 ($n=13$), 0.179 ± 0.011 ($n=14$),

0.176 ± 0.007 ($n=12$), 0.182 ± 0.010 ($n=17$), and 0.176 ± 0.013 ($n=18$), respectively. A grand average for $^{240}\text{Pu}/^{239}\text{Pu}$ of 0.177 and a standard deviation of 0.012 ($n=81$) were determined from the collective core intervals. These values are in good agreement with the reported $^{240}\text{Pu}/^{239}\text{Pu}$ in southern Equatorial (0–30°S) fallout reported by (Kelley et al., 1999), who determined an average $^{240}\text{Pu}/^{239}\text{Pu}$ of 0.173 and a 2σ error of ± 0.027 ($n=8$).

While generalizations about sediment mixing can be made from $^{210}\text{Pb}_{\text{ex}}$ profiles it is best to confirm sediment accumulation rates with additional tracers since both sediment mixing and variation in sedimentation rates can cause the same gradients in $^{210}\text{Pb}_{\text{ex}}$ concentration–depth profiles. Sediment mixing by benthic macrofauna in the subsurface layers may cause an over estimation in sedimentation rates (Santschi and Rowe, 2008) and thus, the need to confirm with additional tracers. In the present case, due to the comparable sedimentation rates determined from $^{210}\text{Pb}_{\text{ex}}$ and $^{239+240}\text{Pu}$ models, sediment mixing produces only a minor influence on the sediment accumulation rates. The $^{210}\text{Pb}_{\text{ex}}$ and $^{239+240}\text{Pu}$ inventories are taken from approximately 1954, except for cores 13 and 15. As cores 13 and 15 do not reach 1954, the inventories and fluxes are based on the entire core, i.e., near 1958 and 1976, respectively. Even though some inventories are incomplete, all $^{210}\text{Pb}_{\text{ex}}$ and $^{239+240}\text{Pu}$ profiles are useful for validating the two independent sediment dating methods. Accordingly, the $^{210}\text{Pb}_{\text{ex}}$ and $^{239+240}\text{Pu}$ fluxes varied, being the highest at Station 15 and the lowest at Station 12 (Table 2).

5. Discussion

5.1. Organic matter composition

As organic material deposited on continental shelves may have differing origins, specific geochemical proxies such as $\delta^{13}\text{C}$ and TOC/TN molar ratios are often used to determine source (Muller-Karger et al., 2005; Niggemann et al., 2007; Santschi et al., 2001). The $\delta^{13}\text{C}$ isotopic composition of marine OC is typically in the range of -22 to -19‰ whereas terrestrial OM from C3 plant photosynthesis varies from -28 to -26‰ (Meyers, 1994) and references therein). The $\delta^{13}\text{C}$ values found here indicate a dominant marine source of the OC deposition.

The TOC/TN molar ratios were between 8 and 10. These ratios are slightly higher than would be expected for marine OM deposited on shelf sediments. Freshly produced planktonic OM, typically rich in protein, has TOC/TN molar ratios between 5 and 7, while terrestrial TOC/TN would generally be well above 12 (Emery and Uchupi, 1984; Meyers, 1994). An explanation for the higher TOC/TN molar ratios, in particular towards the center of the shelf, may be the preferential degradation of N containing compounds during early diagenesis which would result in higher TOC/TN ratios. Higher TOC/TN molar ratios indicate that the sediments may be influenced by ongoing degradation or may be related to the constant action of the Cabo Frio stationary eddy located in this same area (Calado et al., 2008). Despite the small divergences between the organic matter proxies within specific regions of the continental shelf, it is important to note that the data suggests mostly marine origin of the OC deposition. Indeed, when the values of $\delta^{13}\text{C}$ are plotted against TOC/TN ratios, the scatter plots lie in a cluster that is typical of marine plankton (Fig. 4) (Meyers, 1994).

5.2. Particle reactive tracers

Upwelling areas on continental shelves or coastal areas with lateral transport of suspended particles typically have substantially higher sediment accumulation rates compared to deep sea

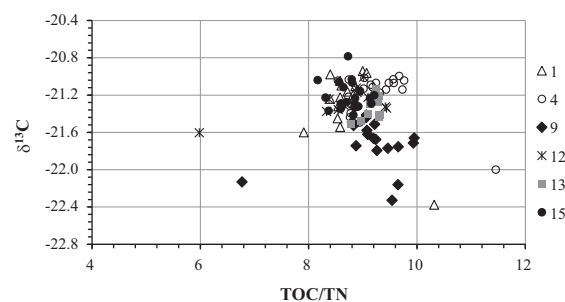


Fig. 4. Sediment $\delta^{13}\text{C}$ values plotted against TOC/TN ratios demonstrate that all samples fall within the marine algae range (Meyers, 1994).

oceanic rates (Anderson et al., 1983; Taguchi et al., 1989). Lateral transport of particle reactive species such as ^{210}Pb and $^{239+240}\text{Pu}$ into regions of deposition leads to the increased flux of these radionuclide tracers (DeMaster et al., 1986; Dukat and Kuehl, 1995; Niggemann et al., 2007; Smoak et al., 1996). The $^{210}\text{Pb}_{\text{ex}}$ inventories, shown in Table 2, give an integrated view of shelf dynamics, as the $^{210}\text{Pb}_{\text{ex}}$ inventories vary greatly from one station to another, indicating a differing depositional flux along the shelf. The $^{210}\text{Pb}_{\text{ex}}$ flux to the shelf sediments is a function of the total supply to the water column from multiple sources. The $^{210}\text{Pb}_{\text{ex}}$ input from the atmosphere, in situ production, continental runoff and offshore waters should be included when considering the sources of the $^{210}\text{Pb}_{\text{ex}}$ to the sedimentation inventories (Smoak et al., 1996). The relatively large fluxes of $^{210}\text{Pb}_{\text{ex}}$ greatly exceeds sediment cores collected in shallow coastal areas where atmospheric supply would be the dominant source (Breithaupt et al., 2012; Sanders et al., 2012). Also, Sanders et al. (2011) measured direct atmospheric fallout rates ($15.3 \text{ mBq cm}^{-2} \text{ yr}^{-1}$) in a coastal site near Cabo Frio. The atmospheric flux from Sanders et al. (2011), which was influenced by continental sources, are likely an overestimate to what is supplied to the continental shelf. Hence, the depositional inventory at the sediment coring locations in this work is far greater than the inventory of the directly deposited atmospheric flux.

The ^{226}Ra concentration in the ocean water off the coast of Rio de Janeiro was found to be near 1.3 mBq kg^{-1} (Smoak et al., 2012). Considering the flux in each core and assuming complete removal of ^{210}Pb produced by in situ ^{226}Ra in the water column, the maximum ^{210}Pb flux from ^{226}Ra decay is 2.4, 2.9, 3.7, 1.1, 6.7 and $7.2 \text{ mBq cm}^{-2} \text{ yr}^{-1}$ estimated at Stations 1, 4, 9, 12, 13 and 15, respectively. These values are overestimates, as it is unlikely the particulate flux would be high enough to remove 100% of the ^{210}Pb produced by ^{226}Ra . Furthermore, studies have shown less than 50% ^{210}Pb flux from ^{226}Ra decay in the water column (Smoak et al., 2000; and references therein). By dividing the our observed $^{210}\text{Pb}_{\text{ex}}$ core fluxes by the combined estimates of atmospheric and water column values, the contribution of lateral transport is estimated to be greater than the other fluxes by factors of 3.9, 4.1, 4.2, 1.5, 2.3 and 5.3 for Stations 1, 4, 9, 12, 13 and 15, respectively.

As there is no direct river flow to the area (the nearest major river is 150 km to the north), the contribution of this possible source is difficult to estimate. The river or runoff source is likely limited, considering that a river as large as the Amazon only contributes 31% of $^{210}\text{Pb}_{\text{ex}}$ to the continental shelf sediments in coastal upwelling regions (Smoak et al., 1996). As is discussed in (Smoak et al., 2006), it is apparent that $^{210}\text{Pb}_{\text{ex}}$ to continental shelf in coastal upwelling regions is dominated by sources other than atmospheric deposition, in situ production and rivers/runoff. Therefore, lateral transport of particle reactive species such as ^{210}Pb into regions of sediment deposition must be a major control on the relatively high fluxes of these radionuclide tracers. The $^{210}\text{Pb}_{\text{ex}}$ fluxes found in this work are comparable to what has been

Table 3

Characteristics of continental shelf upwelling systems. Organic carbon accumulation rates (CAR) are from the previous century.

Site	Depth (m)	Avg. prim. production (g C m ⁻² yr ⁻¹)	OC (%)	SAR (cm yr ⁻¹)	²¹⁰ Pb flux (mBq cm ² yr ⁻¹)	CAR (mol cm ⁻² yr ⁻¹)
Cabo Frio ^a	~100	188–520 ^b	1–2	0.8–5.5	0.2–0.4	1–8
Gulf California ^c	400–800	100–334	~4	1.9	na	6.7
Chilean Coast ^d	100–1300	269	1–5	1.0–2.6	1.0–88.3	8
Namibia ^f	400–800	300	~5	1.0	na	11.7
Peru ^f	100–1000	269	5–20	2.0–4.5 ^e	na	27.5
Oman ^g	150–1200	300	1–6	na	na	0.8
East China Sea ^h	< 200	200	0.1–1.3	0.06	na	1.2

^a Results from this work.^b Burone et al. (2011).^c Brumsack (1989).^d Niggemann et al. (2007).^e Kriete et al. (2004).^f Böning et al. (2004) and references therein.^g Pedersen et al. (1992).^h Deng et al. (2006).

reported in the upwelling Santa Barbara Basin (Smoak et al., 2000) though considerably less than the Chilean Coast (Niggemann et al., 2007) (Table 3).

The initial atmospheric fallout of ²³⁹⁺²⁴⁰Pu is fairly well known and lower than was found in this study (Kelley et al., 1999). Indeed, ²³⁹⁺²⁴⁰Pu fluxes found here are extremely large for Southeastern Brazil, from 0.20 to 0.43 mBq cm² yr⁻¹ and substantially higher than in a nearby coastal sediment core (~0.10 mBq cm² yr⁻¹) (Sanders et al., 2010). The ²³⁹⁺²⁴⁰Pu fluxes follow the same trend as the ²¹⁰Pb_{ex} fluxes, supporting the assertion of lateral transport contributing to the relatively high fluxes of the particle reactive tracers in specific depositional settings (Paulsen et al., 1999; Santschi et al., 2001).

5.3. Organic carbon accumulation rates

Understanding the processes that control accumulation of OC in sediments from upwelling regions is of significance to the global carbon cycle (Baumgart et al., 2010; Muller-Karger et al., 2005). The upwelling of nutrients in specific regions of continental shelves is a fundamental driver of primary production, (Burone et al., 2011; Smoak, 2010) playing a globally significant role in the coastal ocean carbon cycle (Jahnke et al., 1990). In Cabo Frio, nutrient upwelling directly influences the high level of primary production (Burone et al., 2011). The formation of POC as a result of primary production and the lateral transport of POC (i.e., sediment focusing), plays a vital role in the large CAR at differing rates in site specific depots along continental shelves (Fig. 5). Below we demonstrate how lateral transport is evident in upwelling regions, and show how these processes contribute to the high CAR in the Cabo Frio continental shelf.

Excess ²¹⁰Pb inventories of all the sediment cores in this study exceed the supply of ²¹⁰Pb_{ex} from atmospheric ²¹⁰Pb_{ex} deposition and decay of ²²⁶Ra in the water column, indicating that there is a substantial allochthonous source of ²¹⁰Pb_{ex}. Possible factors other than the SACW upwelling differentiating CAR amongst stations include lateral transport processes such as: the passage of meanders, eddies produced by instabilities of the Brazil Current, vertical transport driven by wind stress curl changes and advection as well as accumulation rates influenced by winnowing of organic rich sediments (Belem et al., 2013; Diaz et al., 2012), of which influence the high levels radioisotope tracers inventories and CAR. Indeed, the culmination of primary production in nutrient rich overlying waters, upwelling and lateral transport, likely support the surficial mud deposition shown in Fig. 1.

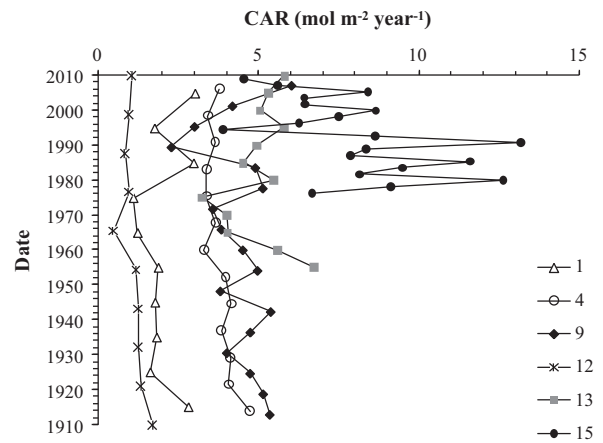


Fig. 5. Organic carbon accumulation rates (mol m⁻² yr⁻¹) based on the ²¹⁰Pb_{ex} dating.

The organic carbon content in the sediments of this study was generally lower than that found in the sediments accumulated during the previous century from the Chilean Coast, the Gulf of California, and Oman (Böning et al., 2005; Brumsack, 1989; Niggemann et al., 2007; Pedersen et al., 1992) which may be directly related to dilution from the high sediment accumulation rates in these regions. As the primary production rates in this work are comparable to other upwelling sites, lateral transport likely differentiates the CAR amongst upwelling regions. Indeed, the extremely high ²¹⁰Pb_{ex} fluxes found by (Niggemann et al., 2007) coincide with the large CARs on the Peruvian continental shelf, indicating that the large ²¹⁰Pb flux is a tracer of high CAR in Peru.

We compare the CAR in this work to other continental shelf areas where upwelling and high-productivity is prevalent, during a time span that covers the previous century (Table 3). The calculated CAR found in this study is similar to the upwelling region off the Gulf of California (Brumsack, 1989) and the Chilean Coast (Böning et al., 2005; Niggemann et al., 2007), though higher than the values in Oman (Pedersen et al., 1992). On the other hand, the average rates found in this work are lower than the CAR from upwelling areas in Namibia (Böning et al., 2004), and substantially lower than along the Peruvian coast (Böning et al., 2004). One of the principal differences in the higher CAR of the Peruvian coast is the greater ²¹⁰Pb flux to the sediments of the upwelling area (Table 3) indicating much higher intensity of lateral transport than

that found in this work. Hence, the upwelling stations with the highest $^{210}\text{Pb}_{\text{ex}}$ and $^{239+240}\text{Pu}$ fluxes, indicating intense lateral transport, are also the sites with the greatest CAR.

6. Conclusion

Sediment deposition along the upwelling region of the continental shelf off Cabo Frio, Brazil was associated with the particle reactive tracers, $^{210}\text{Pb}_{\text{ex}}$ and $^{239+240}\text{Pu}$. The $^{210}\text{Pb}_{\text{ex}}$ and $^{239+240}\text{Pu}$ fluxes indicate large lateral transport to the study region, which is directly related to the relatively high marine CAR (characterized by TOC/TN ratios and $\delta^{13}\text{C}$) in specific depot regions of the shelf. Inventories of $^{210}\text{Pb}_{\text{ex}}$ in all cores exceed the estimated supply of $^{210}\text{Pb}_{\text{ex}}$ from atmospheric deposition and production from ^{226}Ra in the water column. This implies that there is a sufficient supply of suspended particulates to scavenge $^{210}\text{Pb}_{\text{ex}}$, $^{239+240}\text{Pu}$ and OC (boundary scavenging) and the focusing of organic rich sediments to this study region, both of these processes are considered as lateral transport. This work indicates that $^{210}\text{Pb}_{\text{ex}}$ and $^{239+240}\text{Pu}$ sediment inventories are ideal in quantifying recent CAR and intensity of lateral transport on continental shelves.

Acknowledgments

This work was supported by Grant # 0050.0048388.08.9 from Geochemistry Network (Rede Temática de Geoquímica) of the Petroleum National Agency (Agência Nacional do Petróleo) and Petrobras, in cooperation with Universidade Federal Fluminense (UFF) with FAPERJ and CAPES support, Grant (E-26/101.952/2009), and a Southern Cross University post-doctoral fellowship to Christian J. Sanders. MEK acknowledges support from the Arizona Technology Research and Innovation Fund (TRIF) for the purchase of the quadrupole ICPMS.

Appendix A. Supporting information

Supplementary data associated with this article can be found in the online version at <http://dx.doi.org/10.1016/j.csr.2013.10.009>.

References

- Anderson, R.F., Bacon, M.P., Brewer, P.G., 1983. Removal of ^{230}Th and ^{231}Pa from the open ocean. *Earth Planet. Sci. Lett.* 62, 7–23.
- Antoine, D., André, J.M., Morel, A., 1996. Oceanic primary production 2. Estimation at global scale from satellite (coastal zone color scanner) chlorophyll. *Global Biogeochem. Cycles* 10, 57–69.
- Appleby, P.G., Oldfield, F., 1992. Application of lead-210 to sedimentation studies. In: Ivanovich, M., Harmon, R.S. (Eds.), *Uranium Series Disequilibrium: Application to Earth, Marine and Environmental Science*, 2nd ed. Clarendon Press, Oxford, pp. 731–783.
- Baumgart, A., Jennerjahn, T., Mohtadi, M., Hebbeln, D., 2010. Distribution and burial of organic carbon in sediments from the Indian Ocean upwelling region off Java and Sumatra, Indonesia. *Deep-Sea Res. I: Oceanogr. Res. Pap.* 57, 458–467.
- Belem, A.L., Castela, R.M., Albuquerque, A.L., 2013. Controls of subsurface temperature variability in a western boundary upwelling system. *Geophys. Res. Lett.* 40, 1362–1366.
- Blanco, J.L., Thomas, A.C., Carr, M.E., Strub, P.T., 2001. Seasonal climatology of hydrographic conditions in the upwelling region off northern Chile. *J. Geophys. Res. C: Oceans* 106, 11451–11467.
- Böning, P., Brumsack, H.J., Böttcher, M.E., Schnetger, B., Kriete, C., Kallmeyer, J., Borchers, S.L., 2004. Geochemistry of Peruvian near-surface sediments. *Geochim. Cosmochim. Acta* 68, 4429–4451.
- Böning, P., Cuyper, S., Grunwald, M., Schnetger, B., Brumsack, H.J., 2005. Geochemical characteristics of Chilean upwelling sediments at ~36°S. *Mar. Geol.* 220, 121.
- Breithaupt, J.L., Smoak, J.M., Smith III, T.J., Sanders, C.J., 2012. Mangrove organic carbon burial rates: strengthening the global budget. *Global Biogeochemical Cycles*, 26, GB3011, [10.1029/2012GB004375](https://doi.org/10.1029/2012GB004375).
- Brumsack, H.J., 1989. Geochemistry of recent TOC-rich sediments from the Gulf of California and the Black Sea. *Geol. Rundsch.* 78, 851–882.
- Burone, L., de e Sousa, S.H.M., de Mahiques, M.M., Valente, P., Ciotti, A., Yamashita, C., 2011. Benthic foraminiferal distribution on the southeastern Brazilian shelf and upper slope. *Mar. Biol.* 158, 159–179.
- Calado, L., Gangopadhyay, A., da Silveira, I.C.A., 2008. Feature-oriented regional modeling and simulations (FORMS) for the western South Atlantic: southeastern Brazil region. *Ocean Model.* 25, 48–64.
- Campos, E.J.D., Velhote, D., Da Silveira, I.C.A., 2000. Shelf break upwelling driven by Brazil current cyclonic meanders. *Geophys. Res. Lett.* 27, 751–754.
- Cutshall, N.H., Larsen, I.L., Olsen, C.R., 1983. Direct analysis of ^{210}Pb in sediment-samples: self-absorption corrections. *Nucl. Instrum. Methods Phys. Res.* 206, 309–312.
- DeMaster, D.J., Kuehl, S.A., Nittrouer, C.A., 1986. Effects of suspended sediments on geochemical processes near the mouth of the Amazon River: examination of biological silica uptake and the fate of particle-reactive elements. *Cont. Shelf Res.* 6, 107–125.
- Deng, B., Zhang, J., Wu, Y., 2006. Recent sediment accumulation and carbon burial in the East China Sea. *Global Biogeochemical Cycles* 20.
- Diaz, R., Moreira, M., Mendoza, U., Machado, W., Böttcher, M.E., Santos, H., Belém, A., Capilla, R., Escher, P., Albuquerque, A.L., 2012. Early diagenesis of sulfur in atropical upwelling system, Cabo Frio, southeastern Brazil. *Geology* 40, 879–882.
- Dukat, D.A., Kuehl, S.A., 1995. Non-steady-state ^{210}Pb flux and the use of $^{228}\text{Ra}/^{226}\text{Ra}$ as a geochronometer on the Amazon continental shelf. *Mar. Geol.* 125, 329350.
- Emery, K.O., Uchupi, E., 1984. *The Geology of the Atlantic Ocean*. Springer-Verlag, New York.
- Fischer, G., Ratmeyer, V., Wefer, G., 2000. Organic carbon fluxes in the Atlantic and the Southern Ocean: relationship to primary production compiled from satellite radiometer data. *Deep-Sea Res. II: Top. Stud. Oceanogr.* 47, 1961–1997.
- Jahnke, R.A., Reimers, C.E., Craven, D.B., 1990. Intensification of recycling of organic matter at the sea floor near ocean margins. *Nature* 348, 50–54.
- Kelley, J.M., Bond, L.A., Beasley, T.M., 1999. Global distribution of Pu isotopes and ^{237}Np . *Sci. Total Environ.* 237/238, 483–500.
- Ketterer, M.E., Hafer, K.M., Jones, V.J., Appleby, P.G., 2004. Rapid dating of recent sediments in Loch Ness: inductively coupled plasma mass spectrometric measurements of global fallout plutonium. *Sci. Total Environ.* 322, 221–229.
- Kriete, C., Suckow, A., Harazim, B., 2004. Pleistocene meteoric pore water in dated marine sediment cores off Callao, Peru. *Estuarine, Coastal and Shelf Science* 59, 499–510.
- Meyers, P.A., 1994. Preservation of elemental and isotopic source identification of sedimentary organic matter. *Chem. Geol.* 114, 289–302.
- Moore, W.S., 1984. Radium isotope measurements using germanium detectors. *Nucl. Instrum. Methods* 223, 407–411.
- Muller-Karger, F.E., Varela, R., Thunell, R., Luerssen, R., Hu, C., Walsh, J.J., 2005. The importance of continental margins in the global carbon cycle. *Geophys. Res. Lett.* 32, 1–4.
- Naidu, A.S., Cooper, L.W., Finney, B.P., Macdonald, R.W., Alexander, C., Semiletov, I.P., 2000. Organic carbon isotope ratio ($\delta^{13}\text{C}$) of Arctic Amerasian Continental shelf sediments. *Int. J. Earth Sci.* 89, 522–532.
- Niggemann, J., Ferdelman, T.G., Lomstein, B.A., Kallmeyer, J., Schubert, C.J., 2007. How depositional conditions control input, composition, and degradation of organic matter in sediments from the Chilean coastal upwelling region. *Geochim. Cosmochim. Acta* 71, 1513–1527.
- Paulsen, S.C., List, E.J., Santschi, P.H., 1999. Modeling variability in ^{210}Pb and sediment fluxes near the Whites Point outfalls, Palos Verdes Shelf, California. *Environ. Sci. Technol.* 33, 3077–3085.
- Pedersen, T.F., Shimmield, G.B., N.B., P., 1992. Lack of enhanced preservation of organic matter in sediments under the oxygen minimum on the Oman Margin. *Geochim. Cosmochim. Acta* 56, 545–551.
- Ravichandran, M., Baskaran, M., Santschi, P.H., Bianchi, T.S., 1995. Geochronology of sediments in the Sabine-Neches estuary, Texas, USA. *Chem. Geol.* 125, 291–306.
- Sanders, C.J., Smoak, J.M., Cable, P.H., Patchineelam, S.R., Sanders, L.M., 2011. Lead-210 and Beryllium-7 fallout rates on the southeastern coast of Brazil. *J. Environ. Radioact.* 102, 1122–1125.
- Sanders, C.J., Smoak, J.M., Sanders, L.M., Waters, M.N., Patchineelam, S.R., Ketterer, M.E., 2010. Intertidal mangrove mudflat $^{240+239}\text{Pu}$ signatures, confirming a ^{210}Pb geochronology on the southeastern coast of Brazil. *J. Radioanal. Nucl. Chem.* 283, 593–596.
- Sanders, C.J., Smoak, J.M., Waters, M.N., Sanders, L.M., Brandini, N., Patchineelam, S.R., 2012. Organic matter content and particle size modifications in mangrove sediments as responses to sea level rise. *Mar. Environ. Res.* 77, 150–155.
- Santschi, P.H., Guo, L., Asbill, S., Allison, M., Britt Kepple, A., Wen, L.S., 2001. Accumulation rates and sources of sediments and organic carbon on the PalosVerdes shelf based on radioisotopic tracers (^{137}Cs , $^{239+240}\text{Pu}$, ^{210}Pb , ^{234}Th , ^{238}U and ^{14}C). *Mar. Chem.* 73, 125–152.
- Santschi, P.H., Rowe, G.T., 2008. Radiocarbon-derived sedimentation rates in the Gulf of Mexico. *Deep-Sea Res. II: Top. Stud. Oceanogr.* 55, 25722576.
- Smoak, J.M., 2010. The Amazon Shelf. In: Liu, K.-K., Atkinson, L., Quinones, R., Talaeu-McManus, L. (Eds.), *Carbon and Nutrient Fluxes in Continental Margins: A Global Synthesis*. Springer-Verlag, Berlin, pp. 443–449.
- Smoak, J.M., Demaster, D.J., Kuehl, S.A., Pope, R.H., McKee, B.A., 1996. The behavior of particle-reactive tracers in a high turbidity environment: ^{234}Th and ^{210}Pb on the Amazon continental shelf. *Geochim. Cosmochim. Acta* 60, 2123–2137.

- Smoak, J.M., Krest, J.M., Swarzenski, P.W., 2006. Geochemistry of the Amazon Estuary. In: Wangersky, P.J. (Ed.), Handbook of Environmental Chemistry, vol. 5, Part H. Springer-Verlag, Berlin, pp. 71–90.
- Smoak, J.M., Moore, W.S., Thunell, R.C., 2000. Influence of boundary scavenging and sediment focusing on ^{234}Th , ^{228}Th and ^{210}Pb fluxes in the Santa Barbara Basin. *Estuarine, Coastal Shelf Sci.* 51, 373–384.
- Smoak, J.M., Moore, W.S., Thunell, R.C., Shaw, T.J., 1999. Comparison of ^{234}Th , ^{228}Th , and ^{210}Pb fluxes with fluxes of major sediment components in the Guaymas Basin, Gulf of California. *Mar. Chem.* 65, 177–194.
- Smoak, J.M., Sanders, C.J., Patchineelam, S.R., Moore, W.S., 2012. Radium mass balance and submarine groundwater discharge in Sepetiba Bay, Rio de Janeiro State, Brazil. *J. S. Am. Earth Sci.* 39, 44–51.
- Souto, D.D., de Oliveira Lessa, D.V., Albuquerque, A.L.S., Sifeddine, A., Turcq, B.J., Barbosa, C.F., 2011. Marine sediments from southeastern Brazilian continental shelf: a 1200 year record of upwelling productivity. *Palaeogeogr. Palaeoclimatol. Palaeoecol.* 299, 49–55.
- Sumida, P.Y.G., Yoshinaga, M.Y., Ciotti, Á.M., Gaeta, S.A., 2005. Benthic response to upwelling events off the SE Brazilian coast. *Mar. Ecol. Prog. Ser.* 291, 35–42.
- Taguchi, K., Harada, K., Tsunogai, S., 1989. Particulate removal of ^{230}Th and ^{231}Pa in the biologically productive northern North Pacific. *Earth Planet. Sci. Lett.* 93, 223–232.
- Thunell, R., Benitez-Nelson, C., Varela, R., Astor, Y., Muller-Karger, F., 2007. Particulate organic carbon fluxes along upwelling-dominated continental margins: rate and mechanisms. *Global Biogeochemical Cycles*, 21(1), art. no. GB1022.
- Valentin, J.L., Andre, D.L., Jacob, S.A., 1987. Hydrobiology in the Cabo Frio (Brazil) upwelling: two-dimensional structure and variability during a wind cycle. *Continental Shelf Res.* 7, 77–88.
- Yoshinaga, M.Y., Sumida, P.Y.G., Silveira, I.C.A., Ciotti, Á.M., Gaeta, S.A., Pacheco, L.F.C.M., Koettker, A.G., 2010. Vertical distribution of benthic invertebrate larvae during an upwelling event along a transect off the tropical Brazilian continental margin. *J. Mar. Syst.* 79, 124–133.